ECWS

MDPI

Shear-Thinning Fluid Flow in Variable Aperture Channels

Alessandro Lenci [1] and Vittorio Di Federico [1,*]

[1] Dipartimento di Ingegneria Civile, Ambientale e dei Materiali (DICAM), Università di Bologna Alma Mater Studiorum, Bologna, Italy

* Correspondence: vittorio difederico@unibo.it; Tel.: +39-051-209-3750

Abstract: Non-Newtonian fluid flow in a single fracture is a 3-D nonlinear phenomenon which is often averaged across the fracture aperture and described as 2-D. To capture the key interactions between fluid rheology and spatial heterogeneity, we adopt a simplified geometric model to describe the aperture variability, consisting of adjacent one-dimensional channels with constant aperture, each drawn from an assigned aperture distribution. The flow rate is then derived under the lubrication approximation for the two limiting cases of an external pressure gradient which is parallel/perpendicular to the channels; these two arrangements provide an upper/lower bound to the fracture conductance. The fluid rheology is described via the Prandtl-Eyring shear-thinning model. Novel closed-form results for the flow rate and hydraulic aperture are derived and discussed; different combinations of the parameters describing the fluid rheology and the variability of the aperture field are considered. In general, the flow rate depends in a nonlinear fashion on the dimensionless pressure gradient and the distribution parameters.

Keywords: fractured media; flow; variable aperture; non-Newtonian; Prandtl-Eyring

1. Introduction

Non-Newtonian fluid flow in fractured media is of interest in many environmentally related applications, such as hydraulic fracturing, drilling operations, enhanced oil recovery, and subsurface contamination and remediation. The basic building block in fractured media modeling is a thorough understanding of flow and transport in a single fracture [1]. A key concept in single fracture flow and transport is the fracture aperture, defined by the space between the fracture walls. Due to the heterogeneity of these surfaces, the fracture aperture is spatially variable [2,3]. Flow modeling at the single fracture scale leads to determination of the flow rate under a given pressure gradient as a function of the parameters describing the variability of the aperture field or of the confining walls. An hydraulic aperture can then be derived from the flow rate [4], as the aperture of a smooth-walled conduit that would produce the same flow rate under a given pressure gradient as the real rough-walled fracture.

When the fluid behavior is non-Newtonian, the effects of spatial variability are compounded with the influence of rheology, producing striking results, such as pronounced channeling effects [5]. Different constitutive equations were used to represent non-Newtonian behaviour in fracture flow [5,6]. A comprehensive comparison of results for different constitutive equations is still lacking, but the impact of fluid rheology is likely to be significant.

Detailed 2-D or 3-D flow modeling of non-Newtonian flow in single fractures needs to be tackled numerically, with considerable computational effort given the nonlinearity of the flow. Not surprisingly, some authors pursued a simpler approach, with the aim of providing order of magnitude estimates and reference benchmarks for the fracture conductivity. Basically, this approach considers a simplified, extremely anisotropic fracture geometry, with aperture variable along one direction, and costant aperture channels along the other. The arbitrary orientation of the external pressure gradient with respect to the channels gives rise to two limit cases: i) the parallel arrangement, which provides an upper bound to the conductivity, and ii) the serial arrangement,

which provides a lower bound. Flow in an isotropic aperture field is then addressed considering the fracture as a random mixture of elements in which the fluid flows either transversal or parallel to the aperture variation. The hydraulic aperture is derived by a suitable averaging procedure [7].

The present paper follows this avenue of research exploring the impact of a classical, two-parameter shear-thinning constitutive equation, the Prandtl-Eyring model [8], which overcomes the unrealistic behaviour of the power-law model, having infinite apparent viscosity for zero shear rate. Section 2 derives the flow rate under an assigned external pressure gradient for flow of a Prandtl-Eyring fluid in a parallel plate fracture. Section 3 presents the simplified geometry adopted, derives general expressions of the flow rate for flow parallel or perpendicular to constant aperture channels, and proposes a method to evaluate the hydraulic aperture for the 2-D case. Section 4 introduces a specific probability distribution function for the aperture, the gamma distribution, and illustrates corresponding results for the flow rate and hydraulic aperture.

2. Prandtl-Eyring fluid flow in constant aperture fracture

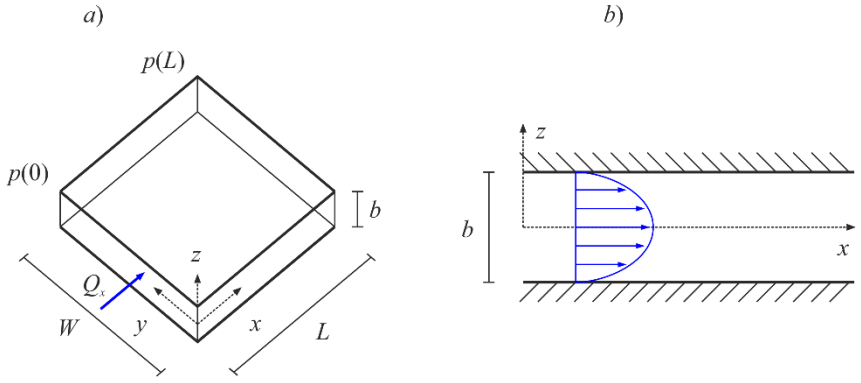

Figure 1. Parallel-plate model: **(a)** model rappresentation and **(b)** cross-sectional velocity profile.

We consider the flow of a non-Newtonian Prandtl-Eyring fluid between two smooth parallel plates separated by a distance b (fracture aperture); the coordinate system is shown in Figure 1. A uniform pressure gradient $\bar{P}_x = -dP/dx$ is applied in the x direction, where $P = p + \rho g z$ includes gravity effects, p is pressure, g gravity, and ρ fluid density. Assuming flow in the x direction, the velocity v_x is solely a function of z. Momentum balance yields a linear shear stress profile

$$\tau_{zx} = \bar{P}_x [z]. \tag{1}$$

A Prandtl-Eyring fluid is described rheologically in simple shear flow by [8]

$$\tau_{zx} = A \sinh^{-1}\left(-\frac{1}{B}\frac{dv_x}{dz}\right), \tag{2}$$

where τ_{zx} is shear stress, $dv_x/dz = \dot{\gamma}$ shear rate, and the parameters A, B describe the fluid. Figure 2 shows the apparent viscosity $\eta(\dot{\gamma})$, defined by the relationship $\tau_{zx} = \eta(\dot{\gamma})\dot{\gamma}$, as a function of shear rate $\dot{\gamma}$, for realistic parameter values.

Substituting eq. (2) in eq. (1), and integrating with the no-slip condition at the wall $v_x(\mp b/2) = 0$, gives the velocity profile between $z = -b/2$ and $z = +b/2$ as

$$v_x(z) = \frac{AB}{\bar{P}_x}\left[\cosh\left(\frac{\bar{P}_x b}{2A}\right) - \cosh\left(\frac{\bar{P}_x |z|}{2A}\right)\right]. \tag{3}$$

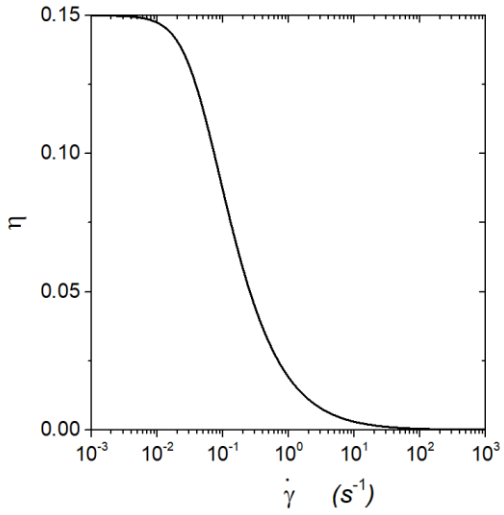

Figure 2. Prandlt-Eyring fluid rheology: shear stress-shear rate relationship. Rheologic parameters from [7]: A=0.00452 Pa and B=0.0301 s^{-1}.

The total flow rate Q_x through the fracture for a width W in the y direction perpendicular to the pressure gradient is derived integrating eq. (2); the result is

$$Q_x = \frac{ABW}{\bar{P}_x}\left[b\cosh\left(\frac{\bar{P}_x b}{2A}\right) - \frac{2A}{\bar{P}_x}\sinh\left(\frac{\bar{P}_x b}{2A}\right)\right];\ q_x = \frac{Q_x}{W};\ V_x = \frac{q_x}{b}, \qquad \text{(4a,b,c)}$$

where q_x is the flow rate per unit width and V_x the average velocity.

If the aperture varies, as in real rock fractures, a flow law of type (4a-b) is valid replacing the constant aperture b with an hydraulic aperture b_H, accounting for the aperture variation [7, 9].

3. Flow in variable aperture channels

Flow and transport simulations in variable aperture fractures typically consider the aperture $b(x,y)$ to vary as a two-dimensional, spatially homogeneous and correlated random field with probability density function $f(b)$ and assigned statistics. The fracture dimensions are assumed to be much larger than the integral scale of the aperture autocovariance function; then, under ergodicity, spatial averages and ensemble averages are interchangeable, and a single realization can be examined [4]. This approach was adopted by [10, 11] to study flow of power-law and truncated power-law fluids in simplified aperture fields where the aperture varies only along one spatial coordinate, and the external pressure gradient, hence the flow, is either transverse or parallele to the aperture variability; such an idealized fracture, of dimensions L and W, is shown in Figure 3.

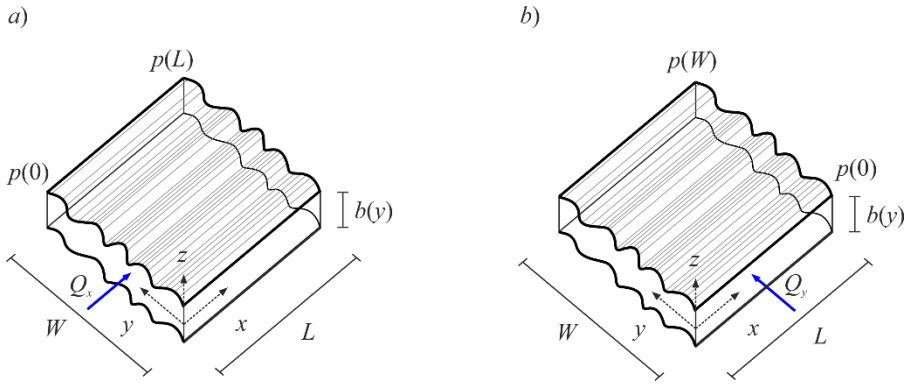

Figure 3. Conceptual model rappresentation: **(a)** parallel arrangement and **(b)** serial arrangement.

3.1. Channels in parallel

Consider flow along the direction x parallel to constant aperture channels, and driven by the external pressure gradient $\bar{P}_x$. To obtain the volumetric flux, a procedure similar to that adopted in [12] is used. The fracture is discretized into N neighboring parallel channels, each having equal width $W_i = W/N$, length L and constant aperture b_i. Assuming that the shear between neighboring channels and the drag against the connecting walls may be neglected, the flow rate in each channel of constant aperture along x is given by eq. (4a) with b_i in place of b and W_i in place of W. Hence summing over all channels the total flow rate in the fracture is

$$Q_x = \sum_{i=1}^{N} Q_{xi} = \frac{ABW}{\bar{P}_x}\frac{1}{N}\sum_{i=1}^{N}\left[b_i \cosh\left(\frac{\bar{P}_x b_i}{2A}\right) - \frac{2A}{\bar{P}_x}\sinh\left(\frac{\bar{P}_x b_i}{2A}\right)\right]. \quad (5)$$

Taking the limit as $N \to \infty$, the width of each channel tends to zero and the discrete aperture variation to a continuous one; then under ergodicity eq. (5) gives for the flow rate per unit width the expression

$$q_x = \frac{Q_x}{W} = \frac{AB}{\bar{P}_x}\left[\int_0^\infty b \cosh\left(\frac{\bar{P}_x b}{2A}\right) f(b)db - \frac{2A}{\bar{P}_x}\int_0^\infty \sinh\left(\frac{\bar{P}_x b}{2A}\right) f(b)db\right], \quad (6)$$

where $f(b)$ is the probability distribution function of the aperture field b, defined between 0 and ∞. Finally, the hydraulic aperture b_{Hx} may be derived numerically upon equating q_x from eq. (6) with eqs. (4a-b) written with b_{Hx} in place of b.

3.2. Channels in series

Consider flow along the direction y parallel to constant aperture channels, and driven by the external pressure gradient $\bar{P}_y$. The fracture, having length W and width L, is discretized into N cells in series of equal length $W_i = W/N$, each of width L and constant aperture b_i. As volumetric flux Q_y through each cell is the same, so is the flow rate per unit width in each cell, i.e. $q_{yi} = q_y = Q_y/L$. The total pressure loss along the fracture in the y direction, ΔP, equals the sum of pressure losses in each cell, ΔP_i , i.e. $\Delta \mathrm{P} = \sum_{\mathrm{i}=1}^{\mathrm{N}} \Delta \mathrm{P_i}$, neglecting the pressure losses due to the succession of constrictions and enlargements. This in turn yields the external mean pressure gradient $\bar{P}_y$ as $\bar{\mathrm{P}}_{\mathrm{y}} = \frac{1}{\mathrm{N}}\sum_{\mathrm{i}=1}^{\mathrm{N}} \mathrm{P_{yi}}$, where the pressure gradient in each cell of constant aperture b_i is given by $P_{yi} = P_{yi}(q_y, b_i, A, B)$ obtained by deriving the pressure gradient as a function of flow rate from eqs. (4a-b), written replacing the subscript x with y and b with b_i. Taking the limit as $N \to \infty$, the length of each cell tends to zero and the discrete aperture variation to a continuous one; then under ergodicity the previous relationship gives for the mean pressure gradient in the y direction

$$\bar{P}_y = \int_0^\infty P_y(q_y, b, A, B) f(b)db. \quad (7)$$

The integration of eq. (7) gives the flow rate as $q_y = q_y(\bar{P}_y, A, B, f(b))$. Finally, the hydraulic aperture b_{Hy} is derived upon equating q_y thus derived with eq. (4b) written with the subscript y in place of x and with b_{Hy} in place of b.

3.3. Flow in 2-D isotropic aperture field

Non-Newtonian flow in a fracture characterized by an isotropic, two-dimensional aperture variation is highly complex [6], and the hydraulic aperture can be obtained only by means of numerical simulations. However, it can be argued [12] that the scheme with channels in parallel is an upper bound to the hydraulic aperture for the general 2-D case, while the scheme with channels in series provides a lower bound, in analogy to hydraulic conductivity [13]. If the fracture is seen as a random mixture of elements where the fluid flows either transversal or parallel to aperture variation, the flow can be approximated by a suitable average of these flows; ergodicity insures that boundary effects are negligible [4]. Hydraulic aperture values derived for the two schemes differ significantly; hence, following the procedure adopted by e.g. [4, 7, 9-12], an estimate of the hydraulic aperture is

derived as the geometric mean of the hydraulic apertures for the parallel and serial arrangement as $b_H = \sqrt{b_{Hx} b_{Hy}}$.

4. Estimate of hydraulic aperture

4.1. Aperture probability distribution

A gamma distribution of shape parameter d and scale parameter b_g, entailing non-negative apertures, is adopted to quantify the previous general expressions, consistently with earlier work [11]. Its probability density function, expected value, variance, and skewness are given by

$$f(b) = \frac{1}{\Gamma(d)} \frac{b^{d-1}}{b_g^d} e^{-b/b_g};\ \langle b \rangle = d b_g;\ \sigma_b^2 = d b_g^2 = \frac{\langle b \rangle^2}{d}, \gamma_b = \frac{2}{\sqrt{d}}, \tag{8a,b,c,d}$$

where $\Gamma(\cdot)$ is the gamma function.

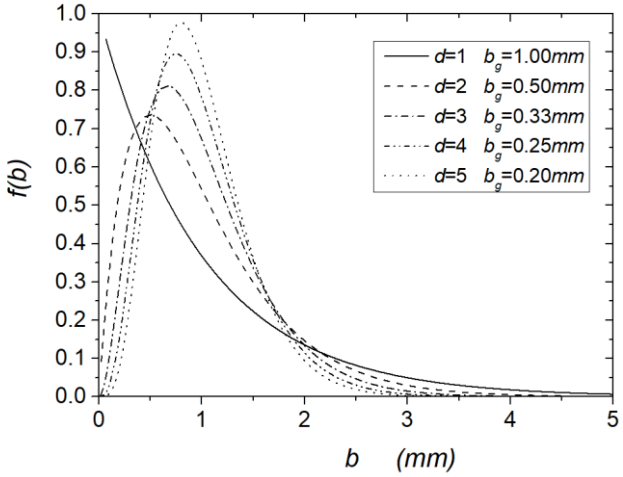

Figure 4. Gamma distribution pdf for different values of the rate parameter d and assuming a mean fracture aperture $\langle b \rangle = 1$ mm.

The gamma distribution is illustrated in Figure 4; for $d = 1$ it reduces to the exponential distribution, with maximum skewness, while as $d \to \infty$, the gamma distribution tends to a normal distribution with the same mean and variance and zero skewness.

4.2. Channels in parallel

Inserting eq. (8a) in eq. (6) gives after integration [14] (p. 403), some algebraic manipulations, usage of eq. (8b), and exploiting the properties of the gamma function, the result

$$q_x = \frac{AB\langle b \rangle}{\bar{P}_x} q_{xD};\ q_{xD} = \frac{1}{2\Omega}\left[\frac{(d+1)u - 1}{(1-u)^{d+1}} + \frac{(d+1)u + 1}{(1+u)^{d+1}}\right], \tag{9a,b}$$

where

$$\Omega = \frac{\bar{P}_x \langle b \rangle}{2A} = \frac{\tau_w}{A};\ u = \frac{\Omega}{d};\ u < 1. \tag{10a,b,c}$$

Eqs. (10b-c) establish that the ratio between the shear stress τ_w at the wall of a parallel plate fracture of aperture $\langle b \rangle$ and the shear stress A describing the fluid cannot exceed the shape parameter d of the distribution. Figure 5 shows the dimensionless flow rate per unit width q_{xD} as a function of Ω for different values of d. As $\Omega \to 0^+$ the flowrate tends to $-\infty$, such negative values are not realistic. On the other hand, for $\Omega \to d$ the flowrate tends to infinity and the curves show a vertical asymptote of equation $\Omega = d$. For low values of Ω, the curves tends to overlap regardless of the value of d. The flow rate strongly depends on the dimensionless pressure gradient and the distribution parameters.

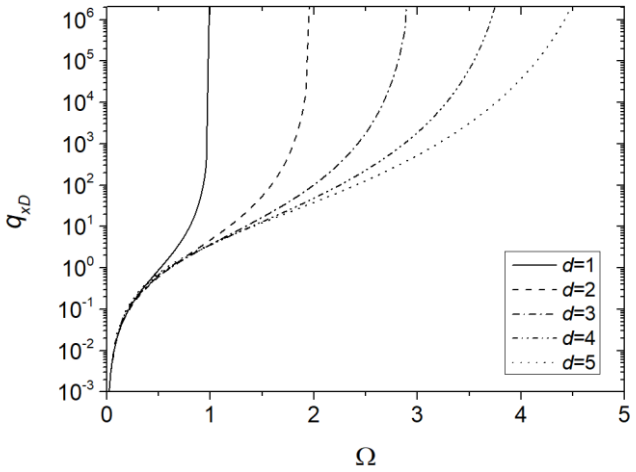

Figure 5. Dimensionless flowrate per unit width q_{xD} versus dimensionless pressure gradient Ω for different values of distribution parameter d.

The hydraulic aperture for the parallel arrangement b_{Hx} is obtained by solving the following implicit equation in the unknown r_x:

$$r_x \cosh(r_x\Omega) - \frac{1}{\Omega}\sinh(r_x\Omega) = \frac{1}{2\Omega}\left[\frac{(d+1)u-1}{(1-u)^{d+1}} + \frac{(d+1)u+1}{(1+u)^{d+1}}\right]; r_x = \frac{b_{Hx}}{\langle b\rangle}. \quad (11a,b)$$

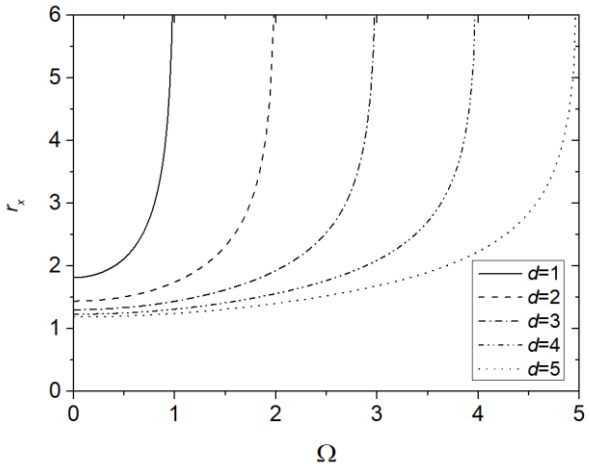

Figure 6. Ratio $r_x = b_{Hx}/\langle b\rangle$ versus dimensionless pressure gradient Ω for different values of the shape parameter d.

Figure 6 illustrates the ratio r_x defined by eqs. (11a-b) as a function of Ω for different values of d. The ratio r_x strongly increases with Ω, more so for lower values of d, i.e. a more skewed distribution. The curves show a vertical asymptote when the dimensionless pressure gradient Ω approaches d. For low values of Ω, the curves are almost horizontal.

Acknowledgments: Vittorio Di Federico gratefully acknowledges financial support from Università di Bologna Almaidea 2017 Linea Senior Grant.

Conflicts of Interest: The authors declare no conflict of interest. The founding sponsor had no role in the design of the study; in the collection, analyses, or interpretation of data; in the writing of the manuscript, and in the decision to publish the results.

References

1. Adler, P.M.; Thovert, J.F.; Mourzenko, V.M. *Fractured Porous Media*. Oxford University Press: Oxford, UK, 2002; pp. 184.
2. Wang, L.; Cardenas, M.B. Analysis of permeability change in dissolving rough fractures using depth-averaged flow and reactive transport models. *Int J Greenh Gas Con* **2019**, *91*, 102824.
3. Meheust, Y.; Schmittbuhl, J. Geometrical heterogeneities and permeability anisotropy of rock fractures. *J Geophys Res* **2001**, 106*(B2)*, 2089-2102.
4. Silliman, S. An interpretation of the difference between aperture estimates derived from hydraulic and tracer tests in a single fracture. *Water Resour Res* **1989**, *25(10)*, 2275-2283.
5. Lavrov, A.. Redirection and channelization of power-law fluid flow in a rough walled fracture. *Chem Eng Sci* **2013**, *99*, 81–88.
6. de Castro, A.R.; Radilla, G. Flow of yield stress and Carreau fluids through rough walled rock fractures: Prediction and experiments. *Water Resour Res* **2017**, 53(7), 6197–6217.
7. Zimmerman, R. W.; Kumar, S.; Bodvarsson, G. S. Lubrication theory analysis of the permeability of rough-walled fractures. *Int. J. Rock Mech. Min. Sci. Geomech. Abstr.* **1991**, 28(4), 325-331.
8. Yoon, H.K.; Ghajar, A.J. A note on the Powell-Eyring fluid model. *Int. Comm. Heat Mass* **1967**, *14*, 381-390.
9. Di Federico, V. Estimates of equivalent aperture for Non-Newtonian flow in a rough-walled fracture. *Int. J. Rock Mech. Min. Sci. Geomech. Abstr.* **1997**, *34(7)*, 1133-1137.
10. Di Federico, V. Non-Newtonian flow in a variable aperture fracture. *Transport Porous Med* **1998**, *30(1)*, 75-86.
11. Felisa, G.; Lenci, A.; Lauriola, I.; Longo, S.; Di Federico, V. Flow of truncated power-law fluid in fracture channels of variable aperture. *Adv Water Resour* **2018**, *122*, 317-327.
12. Zimmerman, R. W; Bodvarsson, G. S. Hydraulic conductivity of rock fractures. *Transport Porous Med* **1996**, 23*(1)*, 1-30.
13. Dagan, G. *Flow and Transport in Porous Formations*; Springer-Verlag: Berlin, Heidelberg, Germany, 1989; pp. 658.
14. Gradshteyn, I. S.; Ryzhik, I. M. *Table of Integrals, Series, and Products*; Academic Press: New York, USA, 1994; pp. 1204.